

# Tevatron combined top quark mass

P. Bartoš<sup>1, a</sup> on behalf of CDF and DØ Collaborations

<sup>1</sup>Faculty of Mathematics, Physics and Informatics, Comenius University - Mlynska Dolina F1 Bratislava 842 48, Slovakia

**Abstract.** We summarize the top-quark mass measurements from the CDF and D0 experiments at Fermilab. We combine published Run I (1992–1996) measurements with the most precise published and preliminary Run II (2001–2012) measurements using a data set corresponding to up to  $8.7 \text{ fb}^{-1}$  of  $p\bar{p}$  collisions. Taking uncertainty correlations into account, and adding in quadrature the statistical and systematic uncertainties, the resulting preliminary Tevatron average mass of the top quark is  $m_t = 173.20 \pm 0.87 \text{ GeV}/c^2$ .

## 1 Introduction

The top quark is the heaviest fundamental particle with the unique properties. It is 3<sup>rd</sup> generation quark with electric charge of  $+2/3e$  and mass of  $173.20 \pm 0.87 \text{ GeV}/c^2$  [1]. The huge mass gives importance to the QCD corrections for the top quark. Due to the very short lifetime ( $\sim 10^{-25} \text{ s}$ ), the top quark decays before hadronization and we can study its properties using its decay products. If we see a deviation of the measured properties from the Standard Model predictions, it could be a sign of new physics. The Yukawa coupling of the top quark is close to unity, what raises the question if it has a special role in the electroweak symmetry breaking. In addition to that the top-quark events are important background in the Higgs-boson studies.

At the Tevatron  $p\bar{p}$  collider, top quarks are produced mainly in pairs through strong force quark-antiquark annihilation ( $\sim 85\%$ ) and gluon-gluon fusion ( $\sim 15\%$ ) processes. As the top quark decays into the  $W$  boson and bottom ( $b$ ) quark in almost 100% of the cases, the final state of top-quark-pair production contains two b-quarks jets and two  $W$  bosons, which decay leptonically (to  $l\nu_l$ , where in our case  $l = e, \mu$ ) or hadronically (into quarks). The  $t\bar{t}$  events can be then classified into three categories: the *dilepton* or *all-jets* events, where both  $W$  bosons decay leptonically or hadronically, respectively; and the *lepton+jets* events, where one of the  $W$  bosons decays leptonically while the other one decays hadronically.

In this article we present the combination of the 12 different top-quark-mass measurements done by the CDF and DØ collaborations using a data set corresponding to up to  $8.7 \text{ fb}^{-1}$ .

## 2 Input measurements

The twelve measurements used in this combination are summarized in Tab. 1.

a. e-mail: bartos.palik@gmail.com

## 2.1 Run I

The first measurements used Run I data (collected from 1992 to 1996) of integrated luminosity of  $0.1 \text{ fb}^{-1}$ . There are tree measurements done by CDF [2–5] and two done by DØ [6, 7] collaboration - all have relatively large statistical uncertainties. Their systematic uncertainties are dominated by the total jet energy scale (JES) uncertainty.

## 2.2 Run II

The measurements, which use Run II data (collected from 2001-2011), are the most recent results in several different decay channels and use up to  $8.7 \text{ fb}^{-1}$  of data. The statistical and systematic uncertainties are reduced by studying much larger  $t\bar{t}$  samples and using new analysis techniques.

### 2.2.1 CDF measurements

The lepton+jets analysis is published result [8], which uses full statistics of collected data ( $8.7 \text{ fb}^{-1}$ ). We constrain the response of light-quark jets using the kinematic information from  $W \rightarrow qq'$  decays (*in situ* calibration) to reduce JES uncertainty. Residual JES uncertainties associated with transverse momenta or pseudo-rapidity dependencies and uncertainties specific to the b-jets response are treated separately. We improved jet energy resolution with respect to the previous combination [9].

The dilepton [10] and all-jets [11] analyses use sample of  $5.6 \text{ fb}^{-1}$  and  $5.8 \text{ fb}^{-1}$ , respectively, and are unchanged with respect to previous combination [9].

The missing-transverse-energy (MET) analysis [12] shows preliminary result updated with  $8.7 \text{ fb}^{-1}$  of data (full data set). In this analysis, events are required to have a missing transverse energy, jets and none identified lepton. The sample is statistically independent from above mentioned three categories and is considered as fourth. The JES uncertainty is also determined by *in situ* calibration.

The analysis based on charged-particle tracking uses  $1.9 \text{ fb}^{-1}$  of data [13]. This technique uses the decay length of B-mesons from  $b$ -jets  $L_{XY}$ . This analysis is almost entirely independent of JES uncertainties, but the statistical sensitivity is not so good as for previously mentioned measurements.

### 2.2.2 $D\bar{0}$ measurements

The two measurements used in this combination include most recent results and are both published.

The lepton+jets measurement [14], based on  $3.6 \text{ fb}^{-1}$  of data, uses JES determined from the external calibration derived from  $\gamma$ +jets events as an additional Gaussian constrain to the *in situ* calibration.

The dilepton analysis [15] uses  $5.4 \text{ fb}^{-1}$  of data. In this case we use JES determined in the lepton+jet measurement by *in situ* calibration.

## 3 Uncertainty Categories

The uncertainties of the measurements are divided into several categories (see [9] for details). The categories are set in such a way, that uncertainties with the same or similar origin are combined (i. e., Signal category below), while some uncertainties have been separated into multiple categories in order to accommodate specific types of correlations (JES uncertainties below).

**In situ light-jet calibration** - originates from *in situ* calibration procedures and is uncorrelated among the measurements. It is part of the JES uncertainty.

**Response to  $b/q/g$  jets** - comes from differences in the detectors response to  $b$ -jets and light-quark jets. It is part of the JES uncertainty.

**Model for  $b$ -jets** - uncertainty, which originates from the  $b$ -jet modeling. It includes uncertainties coming from variations in the semileptonic branching fractions,  $b$ -fragmentation modeling, and differences in the color flow between  $b$ -jets and light-quark jets. It is part of the JES uncertainty.

**Out-of-cone correction** - this part of JES uncertainty is correlated across all measurements. It includes the uncertainties originated in modeling of light-quark fragmentation and out-of-cone corrections.

**Light-jet response (1)** - is specific to the CDF. It includes uncertainties associated with calorimeter response to light-quark jets, multiple interaction and underlying events corrections. This uncertainty is correlated across all CDF measurements independently from the data-taking period (i.e., Run I or Run II). It is uncorrelated between experiments. It is part of the JES uncertainty.

**Light-jet response (2)** - is the uncertainty coming from limitation in the data samples used for calibrations. It is correlated between measurements from the same data-taking period. It is not correlated between experiments. For the CDF, it corresponds to uncertainties associated with the  $\eta$ -dependent JES corrections. For the  $D\bar{0}$  it includes uncertainties coming from calorimeter response to

light jets, uncertainties from  $p_T$ - and  $\eta$ -dependent JES corrections and from the sample dependence of using  $\gamma$ +jets data samples to derive the JES.

**Lepton modeling** - originates from the uncertainties in the scale of the lepton  $p_T$  measurements. It is not treated as a source of systematic uncertainty in the Run I measurements.

**Signal modeling** - is uncertainty arising from  $t\bar{t}$  modeling and is correlated across all measurements. It includes uncertainties from variation of the amount of initial and final state radiation and from the choice of parton density function. For  $D\bar{0}$  it also includes uncertainty from higher order correction (NLO). It also include the uncertainty arising from a variation of color reconnection model (this uncertainty was not evaluated in Run I measurements). Finally, it takes into account the uncertainty coming from the choice of Monte Carlo generator, which is used to  $t\bar{t}$  signal modeling.

**Jet modeling** - arises from uncertainties in the detector modeling in the MC simulation. The  $D\bar{0}$  includes also uncertainties from jet resolution and identification, while these effects were found to be negligible for mass measurements at the CDF.

**Background from theory** - takes care of uncertainty in modeling the background sources. It includes uncertainties of background composition, normalization and shape of different components. It is correlated across all measurements in the same channel.

**Background based on data** - takes into account uncertainties arising from modeling QCD multijets (in lepton+jets, all-hadronic, and MET channel) or Drell-Yan (in dilepton channel) background using data. It is uncorrelated between experiments.

**Calibration method** - comes from any source specific to a particular fit method. It also includes uncertainty arising from using finite MC statistics to the calibration of each method.

**Offset** - is specific to the  $D\bar{0}$ . It comes from uranium noise in the calorimeter and from the multiple interaction correction to the JES. For Run I it was sizable, while for Run II measurements it is negligible.

**Multiple interaction model** - originates in mismodeling of the distribution of the number of collisions per Tevatron bunch crossing. It is uncorrelated between experiments.

All above mentioned systematic uncertainties for each of input measurements are summarize in Tab. 1.

## 4 Combination

The measurements are combined by two independent methods - numerical  $\chi^2$  minimization and the analytic best linear unbiased estimator (BLUE) method [16, 17]. These two methods are mathematically equivalent and give identical results for the combination. The BLUE method yields the decomposition of the uncertainty on the Tevatron combined top-quark mass  $M_t$  in terms of the uncertainty categories specified for the input measurements [17].

For the combination we used following correlations :

**Table 1.** Summary of the measurements used to determine the combined top-quark mass. Integrated luminosity has units of  $\text{fb}^{-1}$ , other numbers are in  $\text{GeV}/c^2$ . Term “n/a” (“n/e”) stands for “not applicable” (“not evaluated”). The total systematic uncertainty and the total uncertainty are obtained by adding the relevant contributions in quadrature.

March 2013												
	Run I published					Run II published					Run II preliminary CDF MEt	
	CDF			DØ		CDF				DØ		
	<i>l</i> +jets	<i>ll</i>	alljets	<i>l</i> +jets	<i>ll</i>	<i>l</i> +jets	<i>ll</i>	alljets	$L_{XY}$	<i>l</i> +jets	<i>ll</i>	
Luminosity	0.1	0.1	0.1	0.1	0.1	8.7	5.6	5.8	1.9	3.6	5.3	8.7
Result	176.1	167.4	86.0	180.1	168.4	172.85	170.28	172.47	166.90	174.94	174.00	173.95
In situ light-jet calibration	n/a	n/a	n/a	n/a	n/a	0.49	n/a	0.95	n/a	0.53	0.55	1.05
Response to <i>b</i> / <i>q</i> / <i>g</i> jets	n/a	n/a	n/a	0.0	0.0	0.09	0.14	0.03	n/a	0.0	0.40	0.10
Model for <i>b</i> jets	0.6	0.8	0.6	0.7	0.7	0.16	0.33	0.15	n/a	0.07	0.20	0.17
Out-of-cone correction	2.7	2.6	3.0	2.0	2.0	0.21	2.13	0.24	0.36	n/a	n/a	0.18
Light-jet response (2)	0.7	0.6	0.3	2.5	1.1	0.07	0.58	0.04	0.06	0.63	0.56	0.04
Light-jet response (1)	3.4	2.7	4.0	n/a	n/a	0.48	2.01	0.38	0.24	n/a	n/a	0.40
Lepton modeling	n/e	n/e	n/e	n/e	n/e	0.03	0.27	n/a	n/a	0.17	0.35	n/a
Signal modeling	2.6	2.9	2.0	1.1	1.8	0.61	0.73	0.62	0.90	0.77	0.86	0.64
Jet modeling	0.0	0.0	0.0	0.0	0.0	0.0	0.0	0.0	0.0	0.36	0.50	0.0
Offset	n/a	n/a	n/a	1.3	1.3	n/a	n/a	n/a	n/a	n/a	n/a	n/a
Background from theory	1.3	0.3	1.7	1.0	1.1	0.12	0.24	0.0	0.80	0.18	0.0	0.0
Background based on data	0.0	0.0	0.0	0.0	0.0	0.16	0.14	0.56	0.20	0.23	0.20	0.12
Calibration method	0.0	0.7	0.6	0.6	1.1	0.00	0.12	0.38	2.50	0.16	0.51	0.31
Multiple interactions model	n/e	n/e	n/e	n/e	n/e	0.07	0.23	0.08	0.0	0.05	0.0	0.18
Systematic uncertainty	5.3	4.9	5.7	3.9	3.6	0.98	3.09	1.49	2.90	1.24	1.44	1.35
Statistical uncertainty	5.1	10.3	10.0	3.6	12.3	0.52	1.95	1.43	9.00	0.83	2.36	1.26
Total uncertainty	7.3	11.4	11.5	5.3	12.8	1.11	3.79	2.06	9.46	1.50	2.76	1.85

- The *Statistical* uncertainty, *Calibration method*, and *In situ light-jet calibration* uncertainties are treated as uncorrelated across the measurements.
- The uncertainties in the *Response to b/q/g jets*, *Light-jet response (2)*, *Lepton modeling*, and *Multiple interaction model* categories are taken to be 100% correlated across all measurements within Run I or Run II. They are treated as uncorrelated between Run I and Run II, and also uncorrelated between the experiments.
- The uncertainties in the *Light-jet response (1)*, *Jet modeling*, and *Offset* categories are taken to be 100% correlated among all measurements within the same experiment. They are treated as uncorrelated between the experiments.
- The *Backgrounds estimated from theory* uncertainties are taken to be 100% correlated across all measurements in the same decay channel.
- The *Backgrounds estimated from data* uncertainties are taken to be 100% correlated among all measurements in the same decay channel and same data-taking period.

They are treated as uncorrelated between the experiments.

- The uncertainties in the *Model for b-jets*, *Out-of-cone correction*, and *Signal modeling* categories are taken to be 100% correlated across all measurements.

By using the inputs measurements and the above mentioned correlations, we obtain the matrix of total correlation coefficients, which is shown in Table 2. The pull and weight for each of the inputs measurements are listed in Table 3. The weights of some measurements are negative, what means that the correlation between two measurements is larger than the ratio of their total uncertainties. In such a case the less precise measurement is assigned by a negative weight. Weight of zero would mean that a input measurement is ignored in the combination. Negative weight means that it affects the resulting combined value and helps reduce the total uncertainty.

We show the absolute values of the weight of each measurement divided by the sum of the absolute values of the weights of all input measurements in Figure 1 to give a better picture of the weights.

**Table 2.** The matrix of correlation coefficients used to determine the Tevatron combined top-quark mass.

March 2013

	Run I published					Run II published					Run II preliminary CDF MEt	
	CDF			DØ		CDF				DØ		
	<i>l</i> +jets	<i>ll</i>	alljets	<i>l</i> +jets	<i>ll</i>	<i>l</i> +jets	<i>ll</i>	alljets	$L_{XY}$	<i>l</i> +jets		<i>ll</i>
CDF Run I, <i>l</i> +jets	1.00	0.29	0.32	0.26	0.11	0.49	0.54	0.25	0.07	0.21	0.12	0.27
CDF Run I, <i>ll</i>	0.29	1.00	0.19	0.15	0.08	0.29	0.32	0.15	0.04	0.13	0.08	0.17
CDF Run I, all-hadronic	0.32	0.19	1.00	0.14	0.07	0.30	0.38	0.15	0.04	0.09	0.06	0.16
DØ Run I, <i>l</i> +jets	0.26	0.15	0.14	1.00	0.16	0.22	0.27	0.12	0.05	0.14	0.07	0.12
DØ Run I, <i>ll</i>	0.11	0.08	0.07	0.16	1.00	0.11	0.13	0.07	0.02	0.07	0.05	0.07
CDF Run II, <i>l</i> +jets	0.49	0.29	0.30	0.22	0.11	1.00	0.48	0.29	0.08	0.30	0.18	0.33
CDF Run II, <i>ll</i>	0.54	0.32	0.38	0.27	0.13	0.48	1.00	0.25	0.06	0.11	0.07	0.26
CDF Run II, all-jets	0.25	0.15	0.15	0.12	0.07	0.29	0.25	1.00	0.04	0.16	0.10	0.17
CDF Run II, $L_{XY}$	0.07	0.04	0.04	0.05	0.02	0.08	0.06	0.04	1.00	0.06	0.03	0.04
DØ Run II, <i>l</i> +jets	0.21	0.13	0.09	0.14	0.07	0.30	0.11	0.16	0.06	1.00	0.39	0.18
DØ Run II, <i>ll</i>	0.12	0.08	0.06	0.07	0.05	0.18	0.07	0.10	0.03	0.39	1.00	0.11
CDF Run II, MEt	0.27	0.17	0.16	0.12	0.07	0.33	0.26	0.17	0.04	0.18	0.11	1.00

**Table 3.** The pull and weight for each of the input measurements used to determine the Tevatron combined top-quark mass.

March 2013

	Run I published					Run II published					Run II preliminary CDF MEt	
	CDF			DØ		CDF				DØ		
	<i>l</i> +jets	<i>ll</i>	alljets	<i>l</i> +jets	<i>ll</i>	<i>l</i> +jets	<i>ll</i>	alljets	$L_{XY}$	<i>l</i> +jets		<i>ll</i>
Pull	+0.40	-0.51	+1.11	+1.32	-0.38	-0.51	-0.82	-0.41	-0.67	+1.42	+0.30	+0.45
Weight [%]	-4.7	-1.1	-0.9	+0.4	-0.2	+62.0	-0.3	+10.5	+0.22	+20.6	+1.4	+11.9

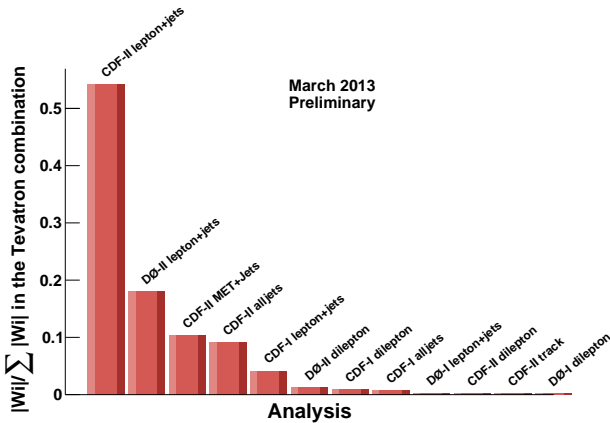


**FIGURE 1.** Relative weights of the input measurements in the combination.

## 5 Results

The value of the combined top-quark mass is  $173.20 \pm 0.51(\text{stat}) \pm 0.71(\text{syst}) \text{ GeV}/c^2$ . The total uncertainty obtained by adding the statistical and systematic uncertainties in quadrature is  $0.87 \text{ GeV}/c^2$ , what corresponds to a relative precision of 0.50%. It has a  $\chi^2$  of 8.5 for 11 degrees of freedom, what corresponds to a probability of 67%. It indicates good agreement among all input measurements. No input has an anomalously large pull (see Table 3).

The total statistical and systematic uncertainties are slightly smaller with respect to the last published combination [9] due to the using full data set in CDF lepton+jets and MEt measurements and due to the improvements in

the treatment of JES corrections. The inputs measurements and the final combined top-quark mass are shown in Fig. 2.

### 5.1 Cross-checks

As a cross-check, we use the same methodology (inputs, uncertainty categories, and correlations) to determine the top-quark mass in the all-jets ( $M_t^{\text{all-jets}}$ ), *l*+jets ( $M_t^{l+\text{jets}}$ ), *ll* ( $M_t^{ll}$ ), and MEt ( $M_t^{\text{MEt}}$ ) channels, separately. The results of these combinations are shown in Table 4. After expressing a  $\chi^2$  probabilities, they indicate that all decay channels are consistent with one other.

**Table 4.** Summary of the calculation of the mass of the top quark in four different decay channels.

March 2013

Parameter	Value ( $\text{GeV}/c^2$ )	Correlation			
		$M_t^{\text{all-jets}}$	$M_t^{l+\text{jets}}$	$M_t^{ll}$	$M_t^{\text{MEt}}$
$M_t^{\text{all-jets}}$	$172.7 \pm 1.9$	1.00			
$M_t^{l+\text{jets}}$	$173.2 \pm 0.9$	0.25	1.00		
$M_t^{ll}$	$170.0 \pm 2.1$	0.19	0.41	1.00	
$M_t^{\text{MEt}}$	$173.8 \pm 1.8$	0.13	0.26	0.18	1.00

In order to check how the choice of the correlation affect our result, we do a cross-check by changing all non-diagonal correlation coefficients of the correlation matrix (Table 2) 100% to 50% and re-calculate the combination. The result from this test is a  $0.19 \text{ GeV}/c^2$  shift of the top-quark mass and a  $0.03 \text{ GeV}/c^2$  decrease of the total uncertainty.

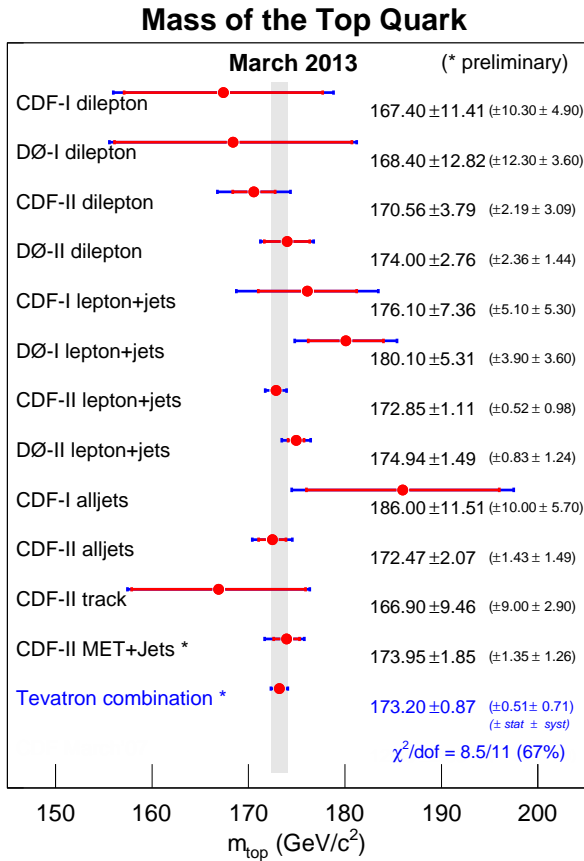


**FIGURE 2.** Overview of the top-quark-mass measurements at the Tevatron and the result of their combination.

We also express two separate combinations of all the CDF and all the DØ measurements, separately. The results of these combinations are  $172.72 \pm 0.93 \text{ GeV}/c^2$  for CDF and  $174.89 \pm 1.42 \text{ GeV}/c^2$  for DØ measurements. We also calculate the  $\chi^2(\text{CDF-DØ}) = 2.25/1$  corresponding to a probability of 13%.

## 6 Conclusion

A preliminary combination of top-quark mass measurements from the CDF and DØ experiments is presented. The combination is based on the five published Run I measurements, six published Run II measurements and one preliminary Run II measurement. Taking into account the statistical and systematic uncertainties and their correlations, the preliminary combined results is  $M_t = 173.20 \pm 0.51(\text{stat}) \pm 0.71(\text{syst}) \text{ GeV}/c^2$  or  $M_t = 173.20 \pm$

$0.87 \text{ GeV}/c^2$ , what corresponds to a relative precision of 0.50% on the top-quark mass. The result is limited by the systematic uncertainties, which are dominated by the jet energy scale uncertainty.

## 7 Acknowledgments

It is a pleasure to thank the CDF and DØ collaborators for their well-done work, the top-group conveners for their help and the organizers of the LHCP 2013 for a very interesting conference.

## References

- [1] Tevatron EW Working Group, CDF and DØ Collaborations, arXiv :1305.3929 [hep-ex]
- [2] F. Abe *et al.* (CDF Collaboration), Phys. Rev. Lett. **82** 271 (1999), arXiv :9810029 [hep-ex]
- [3] F. Abe *et al.* (CDF Collaboration), Phys. Rev. Lett. **82** 2808 (1999), arXiv :9810029 [hep-ex]
- [4] T. Aaltonen *et al.* (CDF Collaboration), Phys. Rev. D **63** 032003 (2001), arXiv :0006028 [hep-ex]
- [5] F. Abe *et al.* (CDF Collaboration), Phys. Rev. Lett. **79** 1992 (1997)
- [6] B. Abbott *et al.* (DØ Collaboration), Phys. Rev. D **60** 052001 (1999), arXiv :9808029 [hep-ex]
- [7] V. M. Abazov *et al.* (DØ Collaboration), Nature **429** 638 (2004), arXiv :0406031 [hep-ex]
- [8] T. Aaltonen *et al.* (CDF Collaboration), Phys. Rev. Lett. **109** 152003 (2012)
- [9] T. Aaltonen *et al.* (CDF and DØ Collaborations), Phys. Rev. D **86** 092003 (2012)
- [10] T. Aaltonen *et al.* (CDF Collaboration), Phys. Rev. D **81** 032002 (2010), Phys. Rev. D **83** 111101 (2011), arXiv :1105.0192 [hep-ex]
- [11] T. Aaltonen *et al.* (CDF Collaboration), Phys. Lett. B **714**, 24 (2012)
- [12] T. Aaltonen *et al.* (CDF Collaboration), CDF Conference Note 10433
- [13] T. Aaltonen *et al.* (CDF Collaboration), Phys. Rev. D **81** 032002 (2010)
- [14] V. M. Abazov *et al.* (DØ Collaboration), Phys. Rev. D **84** 032004 (2011)
- [15] V. M. Abazov *et al.* (DØ Collaboration), Phys. Rev. D **86** 051103 (2012)
- [16] L. Lyons, D. Gibaut, and P. Clifford, Nucl. Instrum. Meth. A **270** 110 (1988)
- [17] A. Valassi, Nucl. Instrum. Meth. A **500** 391 (2003)